UDC 537.311.1:541.182.023.4

DOI: 10.15372/CSD2021331

Platinum-Rich Solid Solution in Nanostructured FePt System

N. S. ZAKHAROV[1], V. M. PUGACHEV[1,2], YU. A. ZAKHAROV[1], A. N. POPOVA[1]

[1]*Federal Research Centre of Coal and Coal Chemistry, Siberian Branch of the Russian Academy of Sciences, Kemerovo, Russia*

E-mail: 2metil4@gmail.com

[2]*Kemerovo State University, Kemerovo, Russia*

Abstract

Features of phase formation and properties of solid solutions in the nanostructured FePt system synthesized by reducing the aqueous solutions of precursors by hydrazine hydrate are considered. It is established by means of X-ray diffraction studies and elemental analysis involving optical emission spectroscopy that limited solid solutions with the fcc type structure are formed under the conditions of the samples with the component ratio Pt/Fe ≥ 0.5. With iron content (C_{Fe}) ≤ 11.6±0.7 at. %, the system is monophase (an fcc-solid solution), with higher iron content it is composed of two phases (an fcc-solid solution with C_{Fe} = 11.6±0.7 at. % and a diffraction-invisible phase relatively enriched with iron). The size of the coherent scattering region for the solid solution varies from 7 to 9 nm. The presence of Fe^{3+} was revealed in all samples by means of electron paramagnetic resonance. Small amounts of iron hydroxide and oxides were detected by means of XRD in the samples with a high iron content. The temperature regions of O_2 and CO_2 desorption, thermal decomposition of extrinsic FeO(OH) and crystallite agglomeration accompanied by phase transformations were determined in the studies of thermally stimulated processes.

Keywords: nanoparticles, solid solution, FePt, XRD, elemental analysis, electron paramagnetic resonance

INTRODUCTION

Urgent problems of electronics and magnetotecnics to be solved require materials with high magnetic characteristics. Systems based on bimetallic nanoparticles FePt, CoPt, FePd, CoPd belong to hard-magnetic with record-breaking coercivity due to their giant magnetic anisotropy resulting from crystal formation in the form of highly ordered tetragonal structure $L1_0$ [1–9].

One of the widely used methods to obtain nanostructured FePt systems is in the joint reduction of the aqueous solutions of precursors. Investigation of the phase composition of this system is an essential task in solving the problem of the formation of highly ordered phase $L1_0$ [10, 11].

It is known [1–8] that platinum is reduced faster than iron during the joint reduction of $PtCl_6^{2-}$ and Fe^{2+} ions because of the higher oxidation-reduction potential [12–14], and finally, a disordered phase $A1$ is formed, with face-centred cubic (fcc) lattice, even in spite of the phase diagram. The transformation of phase $A1$, observed by means of X-ray phase analysis (XPA) [11, 12], into ordered phases $L1_0$ or $L1_2$ (intermetallides) proceeds during heating as a result of sequential series of solid-phase processes (reactions) participated by nanophases enriched with iron to different extents.

In the present work, we chose the aqueous solution of hydrazine hydrate ($N_2H_4 \cdot H_2O$) with pH > 12 as a reducing agent because the products of the reduction of the aqueous solutions of precursors, in this case, are molecular nitrogen and water. So, the resulting nanoparticles are not contaminated with the by-products of reduction. The absence of surfactants and by-products of reduction makes this method of the synthesis of FePt

nanoparticles promising, in particular for biomedical purposes.

The present work is a continuation of the studies carried out by the authors in the area of synthesis and investigation of nanostructures bimetal particles and deals with the investigation of the effect of the chemical composition of FePt particles on their phase composition.

EXPERIMENTAL

Materials and sample synthesis

The reagents that were used to synthesize FePt nanoparticles include $FeSO_4 \cdot 7H_2O$ (chemically pure grade), $H_2[PtCl_6]$ (analytically pure grade), $N_2H_4 \cdot H_2O$ (analytically pure grade), NaOH (chemically pure grade), isopropyl alcohol. The synthesis was carried out by means of the joint reduction of precursor mixtures (in the concentration of 0.1 mol/L) in twice distilled water in an open thermostatic reactor at 90 °C equipped with a top-drive mechanical mixer. The necessary amounts of precursor solutions (depending on the required amount and composition of the target product) were poured into the reactor sequentially, then the reducing agent (an aqueous solution of $N_2H_4 \cdot H_2O$ with pH > 12) was added with an increase in mixing rate. The resulting suspension was centrifuged many times and washed with distilled water. Then, to remove residual water, centrifuging in isopropyl alcohol was carried out. Thus obtained powder composed of nanoparticles was dried at room temperature in the air. This procedure was used to obtain FePt nanoparticles with the calculated ratios $Fe_{10}Pt_{90}$, $Fe_{19}Pt_{81}$, $Fe_{24}Pt_{76}$, $Fe_{48}Pt_{52}$, $Fe_{70}Pt_{30}$. According to the Fe–Pt phase diagram [15], these ratios correspond to the major phase regions of the system: iron content 10, 19 at. % corresponds to the solid fcc solution, iron content 24 at. % – to the two-phase region solid solution – $FePt_3$ intermetallide, iron content 48 at. % – FePt intermetallide, iron content 70 at. % –Fe_3Pt intermetallide.

Investigation methods

The elemental analysis of the samples was carried out by means of optical emission spectroscopy (OES) with inductively coupled plasma using an iCAP 6500 DUO spectrometer (Thermo Scientific, USA) with plasma observation in the radial mode [16].

The XPA data for the samples were obtained with a powder diffractometer D8 ADVANCE A25 (Bruker, Germany) at room temperature in CuK_α-radiation (λ = 1.5406 Å, Ni-filter at the secondary beam) within the angle range of 15–130° over 2θ, with the scanning step of 0.02°. Data collection and diffraction patterns processing were carried out using a Diffrac.Suite.Eva software package (V3.1).

Thermally stimulated processes were studied by means of differential scanning calorimetry (DSC) combined with thermogravimetry (TG) and mass spectrometric investigation of the released products' decomposition with the help of a synchronous thermal analyzer STA 409 PG Luxx (Netzsch, Germany).

Investigation of the samples by means of electron paramagnetic resonance (EPR) was performed with the EMX Micro 6/1 spectrometer (Bruker, Germany) in a rectangular resonator at room temperature (the power of the microwave generator was 1.529 mW, modulation frequency 100 kHz, modulation amplitude 4 G).

RESULTS AND DISCUSSION

It was established by means of elemental analysis that the calculated (required) component content practically corresponds to the determined one. Analysis results are presented in Table 1. All the samples were subjected to extended elemental analysis for the presence of impurities. It was determined that the concentrations of impurities in the samples do not exceed the level claimed by the manufacturers of reagents used for the synthesis.

X-ray diffraction patterns of all samples reveal the crystallized fcc phase of the FePt solid solution (Fig. 1). Iron content in the solid solution was determined using the dependence of the molar fraction of Pt (X_{Pt}) in this solid solution on the average volume per 1 metal atom (V_{Pt}) [12]:

$$X_{Pt} = 2.4108 - 0.60677V_{Pt} + 0.033992V_{Pt}^2 \quad (1)$$

Lattice parameters and the compositions of the series of cubic phases represented in the ICDD databases of X-ray diffraction data are used in the equation.

For all samples (except $Fe_{70}Pt_{30}$), thus determined average iron content in the fcc phase of the solid solution is 11.6±0.7 at. % (see Table 1, Fig. 2).

The high Pt content in the solid solution (88–89 at. %) in comparison with the calculated value agrees with the XPA data on the formation of the fcc phase with *A*1 structural type (according to the Fe–Pt phase diagram [15]). The formation

TABLE 1

Lattice parameter and iron content in the sample (total and in the fcc phase)

Sample	Lattice parameter, Å	Fe content, at. %		CSR size, nm
		in solid solution (XPA)	in samples (OES)	
$Fe_{70}Pt_{30}$	3.886±0.002	17.3±0.7	73	6
$Fe_{48}Pt_{52}$	3.900±0.001	11.2±0.5	54	7
$Fe_{24}Pt_{76}$	3.898±0.001	11.9±0.2	28	9
$Fe_{19}Pt_{81}$	3.897±0.001	12.4±0.6	22	7
$Fe_{10}Pt_{90}$	3.890±0.001	10.9±0.6	13	9
Pt (PDF-2)	3.9231	15.095	–	–

Note. CSR is the coherent scattering region; XPA is X-ray phase analysis; OES is optical emission spectroscopy.

of intermetallides with the ordered phase $L1_2$ might be observed in the sample $Fe_{70}Pt_{30}$, however, suprastructural reflections within this composition range are difficult to distinguish because of their extremely low intensity; detection of intermetallides is also hindered by the fluorescence background of iron.

In the sample with the calculated composition $Fe_{10}Pt_{90,}$ iron content in the solid solution is 10.9±0.6 at. % according to XPA, which is the evidence that the sample is monophase ($A1$ phase).

The excess of platinum content in the solid solution in comparison with the calculated components' ratio in other samples shows that they contain, along with the solid solution observed by means of XPA, also an XPA-invisible phase (maybe several phases) with the higher iron content (see Fig. 2, *a, b*). We observed this effect also in other compositions of the nanostructured FePt system obtained under conditions differing from those used in the present work [12, 13, 17].

The size of the coherent scattering regions (CSR) was estimated according to the Scherrer equation to be within the range 6 to 9 nm (see Table 1). It was discovered that the CSR sizes are close to each other in the solid solutions containing the limiting iron concentrations.

No signs of iron oxidation were observed in the samples with iron content less than 50 at. % (according to OES data). The diffraction patterns of the $Fe_{48}Pt_{52}$ and $Fe_{70}Pt_{30}$ samples contain three clearly pronounced reflections at 35.6, 57.20 and 62.9° over 2θ (see Fig. 1) with interplane distances 2.552, 1.610 and 1.478 Å, respectively. According to the data of the ASTM PDF-2 database, these groups of reflections relate to FeO(OH) [18].

A slight overstatement of Fe content, established by means of OES, may be explained by the

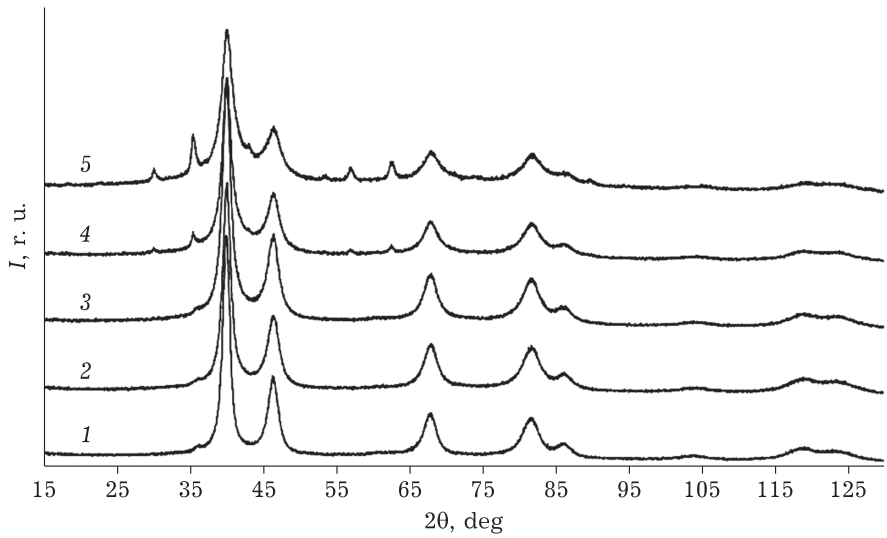

Fig. 1. Diffraction patterns of the samples of FePt nanoparticles: $Fe_{10}Pt_{90}$ (*1*), $Fe_{19}Pt_{81}$ (*2*), $Fe_{24}Pt_{76}$ (*3*), $Fe_{48}Pt_{52}$ (*4*), $Fe_{70}Pt_{30}$ (*5*).

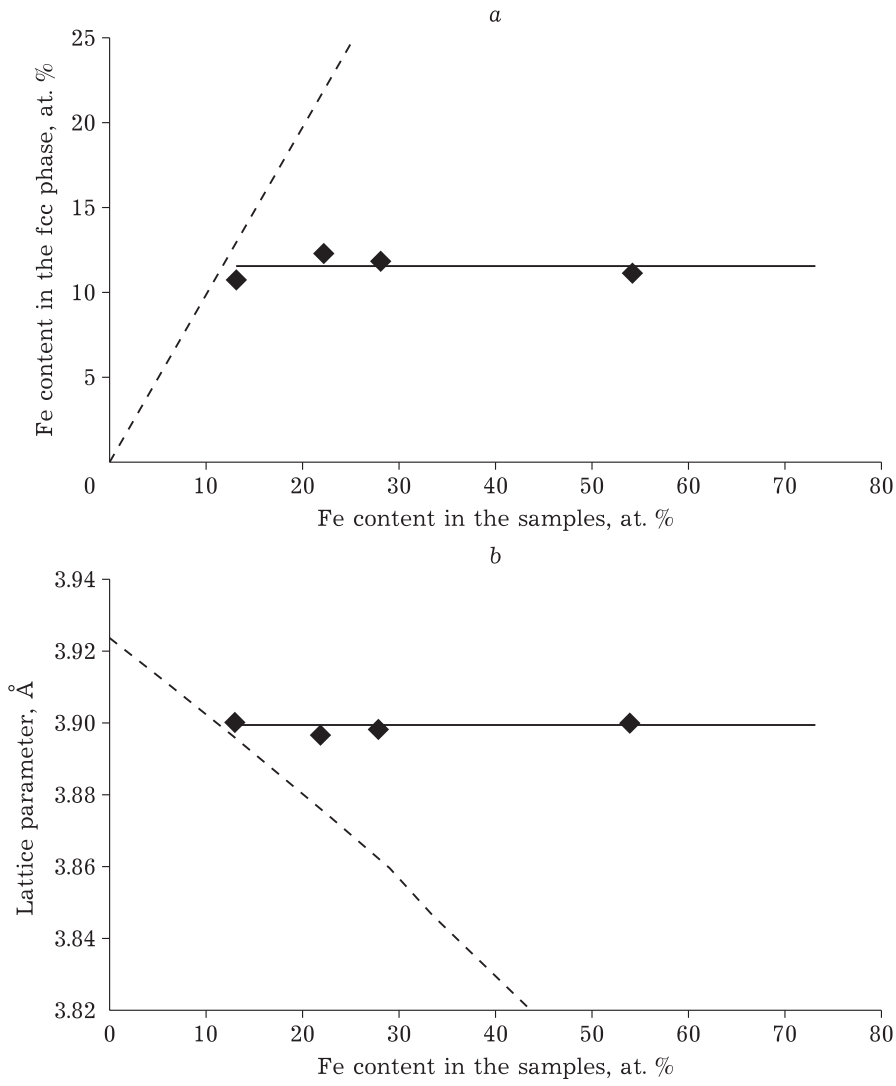

Fig. 2. Dependences of the composition (*a*) and lattice parameter (*b*) of the fcc phase (according to XPA data) on sample composition (according to the results of OES). The plotted values are: *a* – average iron content in the fcc phase of the solid solution in samples without oxide phases (straight line) and Fe content for the hypothetic formation of a single phase of solid solution (dash line); *b* – average lattice parameter in the samples containing no oxide phases (straight line) and hypothetical dependence according to equation (1) (dash line).

presence of oxidized iron in the sample. Determination of oxidized iron by means of diffraction studies is hindered because of the low scattering capacity of iron in comparison with platinum, and a small amount of that phase. To confirm this assumption, the $Fe_{10}Pt_{90}$ sample was studied by means of EPR. The EPR spectrum is shown in Fig. 3; it contains three absorption signals with *g*-factor values 4.18, 2.17 and 2.14. The line of the signal with a *g*-factor equal to 2.14 is a typical curve of ferromagnetic resonance, characteristic of polydisperse highly magnetic particles [19–22]. The presence of a signal with a *g*-factor equal to 4.18 and substantially lower intensity provides a qualitative confirmation of the presence of insignificant amount of high-spin Fe^{3+} ions in the sample [20]. A weak signal with a *g*-factor equal to 2.17 is related to unresolved superfine structure of the EPR spectrum of Mn^{2+} ions. These Mn^{2+} ions are typical admixture ions in iron-containing reagents.

As we have already mentioned above, comparison of the data on the amount of iron in the fcc-phase solid solutions as determined by means of XPA with the results related to a sample as a whole and obtained by means of OES (see Fig. 2) may lead us to the conclusion that the system contains a phase that cannot be detected using

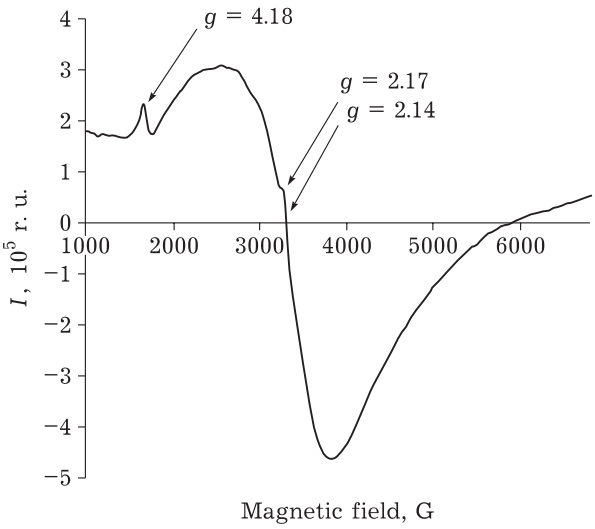

Fig. 3. EPR spectrum of $Fe_{10}Pt_{90}$ nanoparticles.

diffraction-based methods. The coincidence of iron content determined by means of XPA and OES is observed only for the $Fe_{10}Pt_{90}$ sample. This fact confirms the conclusion concerning the existence of the upper limit of iron solubility in platinum in the nano-structured FePt system obtained using the described method.

Thermally stimulated processes in the samples were studied using the combined DSC, TG methods and mass spectrometry of the released products. For instance, a small endo effect is observed as shown in Fig. 4, *a*, *b* in the temperature range 100–150 °C. According to the data of mass spectrometry, this effect is due to O_2 and CO_2 desorption. The endo effect at a temperature of 160–260 °C is most probably due to the thermal decomposition of iron hydroxocarbonates (with the

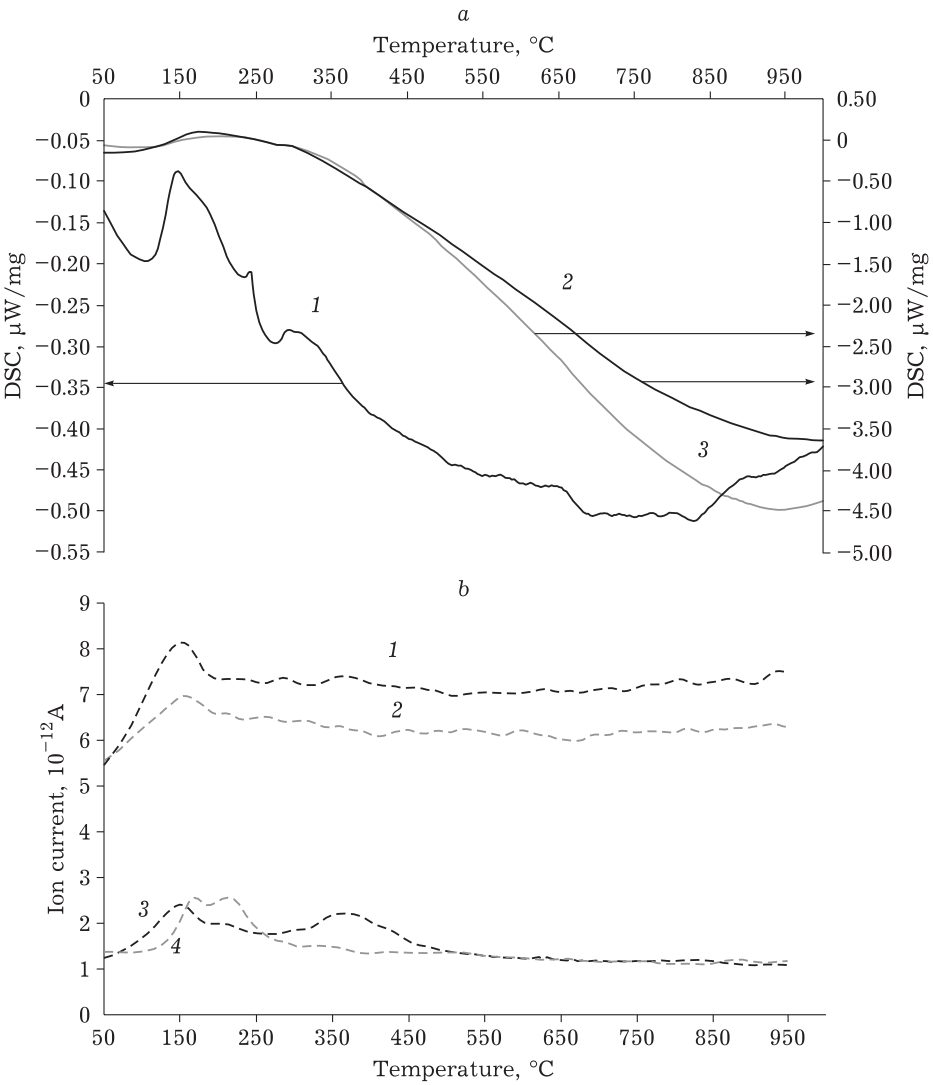

Fig. 4. *a* – DSC curves for $Fe_{10}Pt_{90}$ samples (*1*); $Fe_{48}Pt_{52}$ (*2*) $Fe_{24}Pt_{76}$ (*3*); *b* – mass spectra of the evolved products: H_2O (18 a.m.u.) – samples $Fe_{24}Pt_{76}$ (*1*), $Fe_{48}Pt_{52}$ (*2*); CO_2 (44 a.m.u.) – samples $Fe_{48}Pt_{52}$ (*3*), $Fe_{24}Pt_{76}$ (*4*).

evolution of H_2O and CO_2, according to the results of mass spectrometry), the amount of which is small according to the data of EPR and XPA. A small decrease in sample mass within the indicated temperature regions corresponds to the above-described facts: by 0.1–0.2 mass % during the evolution of H_2O and by 0.2–0.4 mass % during the evolution of CO_2 for the samples of different compositions.

The exo effect at 300–320 °C may be connected with the transformations of iron (III) oxides [23], which are also present in the samples in small amounts, as suggested by the results of XPA. The practical absence of the endo effect on DSC curves of the $Fe_{10}Pt_{90}$ sample may be naturally linked to the monophase nature of this sample and, therefore, to the absence of phase transformations.

A monotonous endothermic effect is recorded in $Fe_{24}Pt_{76}$ and $Fe_{48}Pt_{52}$ samples within a temperature range above 350 °C, which may be related to the aggregation of fine particles with the formation of the new crystal phase (phases) [12].

CONCLUSION

It is established by means of XPA that the phase observed in the nanostructured FePt system obtained through the joint reduction of the aqueous solutions of precursors is a nano-sized solid solution with the limiting iron content 11.6±0.7 at. % and CSR size 7–9 nm. In the samples containing iron in amounts higher than the limiting value, an XPA-invisible phase (phases) richer in iron is formed along with this solid solution. It follows from the EPR data and the comparison between iron content values determined by means of XPA and OES that non-reduced iron (Fe^{3+}) is present in insignificant amounts in the studied samples. Thermal analysis of FePt samples allowed us to determine the temperature regions of gas desorption, thermal decomposition of extrinsic FeO(OH) and possibly the oxides of iron (III), as well as agglomeration of nanocrystals and phase transformations.

Acknowledgements

The work was carried out using the equipment of the Shared Equipment Centre at the FRC CCC SB RAS within the State Assignment for the FRC CCC SB RAS for the years 2021–2023 (Project No. 121031500211-9).

Authors thank Senior Researcher Kolmykov R. P. and Leading Engineer Khitsova L. M. for participation in experiments.

REFERENCES

1 Zaharov Yu. A., Pugachev V. M., Dodonov V. G., Popova A. N., Kolmykov R. P., Rostovtsev G. A., Vasiljeva O. V., Zyzyukina E. N., Ivanov A. V., Prosvirin I. P., Nanosize powders of transition metals binary systems, *J. Phys. Conf. Ser.,* 2012, Vol. 345, Art. 012024.

2 Popova A. N., Zaharov Yu. A., Pugachev V. M., Chemical synthesis, structure and magnetic properties of nanocrystalline Fe-Co alloys, *Mater. Lett.*, 2012, Vol. 74, P. 173–175.

3 Liu Y., Jiang Y., Kadasala N., Zhang X., Mao C., Wang Y., Liu H., Liu Y., Yang. J., Yan Y., Effects of Au on the structure and magnetic properties of $L1_0$-FePt nanoparticles synthesized by the sol–gel method, *J. Solid State Chem.*, 2014, Vol. 215, P. 167–170.

4 Popova A. N., Synthesis and characterization of iron-cobalt nanoparticles, *J. Phys. Conf. Ser.*, 2012, Vol. 345, Art. 012030.

5 Pugachev V. M., Zakharov Yu. A., Popova A. N., Synthesis of nanostructured Fe-Pt system with equiatomic composition, *Butlerov. comm.*, 2017, Vol. 51, No. 8, P. 155-160. (In Russ.).

6 Li D., Poudyal N., Nadwana V., Hard magnetic FePt nanoparticles by salt-matrix annealing, *J. Appl. Phys.*, 2006, Vol. 99, No. 8, Art. 08E911.

7 Rong C. B., Li D., Wang Z., Size-dependent chemical and magnetic ordering in *L*10-FePt nanoparticles, *Adv. Mater.*, 2006, Vol. 18, No. 22, P. 2984–2988.

8 Rellinghaus B., Stappert S., Acet M., Wassermann E. F., Magnetic properties of FePt nanoparticles, *J. Magn. Magn. Mater.,* 2003, Vol. 266, No. 1–2, P. 142–154.

9 Elkins K., Li D., Poudyal N., Nandwana V., Jin Z., Chen K., Liu J. P., Monodisperse face-centred tetragonal FePt nanoparticles with giant coercivity, *J. Phys. D*, 2005, Vol. 38, No. 14, P. 2306–2309.

10 Medwal R., Sehdev N., Fyyapoorni S., Electronic states of self stabilized $L1_0$ FePt alloy nanoparticles, *Appl. Phys. A*, 2012, Vol. 109, P. 403–408.

11 Klemmer T. G., Shukla N., Liu C., Wu X. W., Svedberg E. B., Mrysov O., Chantrel R. W., Weller D., Structural studies of $L1_0$ FePt nanoparticles, *Appl. Phys. Lett.,* 2002, Vol. 81, No. 12, P. 2220–2222.

12 Pugachev V. M., Zakharov Y. A., Popova A. N., Russakov D. M., Zakharov N. S., Phase transformations of the nanostructured iron-platinum system upon heating, *J. Phys. Conf. Ser.,* 2021, Vol. 1749, No. 1, Art. 012036.

13 Zakharov N. S., Popova A. N., Zakharov Y. A., Pugachev V. M., Synthesis of nanostructured FePt systems, *J. Phys. Conf. Ser.,* 2021, Vol. 1749, No. 1, Art. 012012.

14 Zakharov N. S., Popova A. N., Zakharov Y. A., Pugachev V. M., Russakov D. M., Transmission electron microscopy for evaluating the structural parameters of nanoparticles, *J. Phys. Conf. Ser.*, 2021, Vol. 1749, No. 1, Art. 012011.

15 Lyakishev N. P., State Diagrams of Binary Metal Systems. Reference Book in 3 Volumes, Vol. 2. Mechanical Engineering, Moscow, 1997. (In Russ.).

16 Zakharov Y. A., Pugachev V. M., Bogomyakov A. S., Ovcharenko V. I., Korchuganova K. A., Russakov D. M., Kolmykov, R. P., Influence of $Ni_{core}Au_{shell}$ nanoparticles' morphology on their magnetic properties, *J. Phys. Chem. C*, 2019, Vol. 124, No. 1, P. 1008–1019.

17 Zakharov N. S., Popova A. N., Zakharov Yu. A., Grishaeva O. V., Comparison of methods for the synthesis of the nanostructured FePt system, *Butlerov. comm.*, 2020, Vol. 64, No. 10, P. 33–39. (In Russ.).
18 Fleet M. E., The structure of magnetite: Symmetry of cubic spinels, *J. Solid State Chem.*, 1986, Vol. 62, P. 75–82.
19 Nkosi S. S., Gavi H. M., Motaung D. E., Keartland J., Sideras-Haddad E., Forbes A., Mwakikunga B. W., Ferromagnetic resonance characterization of nano-FePt by electron spin resonance, *J. Spectrosc.*, 2012, Vol. 2013, Art. 272704.
20 Tsuruda H., Komorida Y., Mito M., Deguchi H., Takagi S., Iwamoto T., Kitamoto Y., Observation of two kinds of ESR spectra in FePt nanoparticles, *J. Phys. Conf. Ser.*, 2010, Vol. 200, No. 7, Art. 072102.
21 Noginova N., Weaver T., Giannelis E. P., Bourlinos A. B., Atsarkin V. A., Demidov V. V., Observation of multiple quantum transitions in magnetic nanoparticles, *Phys. Rev. B*, 2008, Vol. 77, No. 1, Art. 014403.
22 Ceglia A., Nuyts G., Meulebroeck W., Cagno S., Silvestri A., Zoleo A., Nys K., Janssens K, Thienpont H., Terryn H., Iron speciation in soda-lime-silica glass: A comparison of XANES and UV-vis-NIR spectroscopy, *J. Anal. At. Spectrom.*, 2015, Vol. 30, No. 7, P. 1552–1561.
23 Kotikov D. A., Ivanovskaya M. I., The use of the sol-gel method for the synthesis of various structural modifications of iron (III) oxide in the nanosized state, *Bull. BSU. Ser. 2. Chemistry. Biology. Geography*, 2005, No. 2, P. 11–15. (In Russ.).